Optimizing Template Models to Quantifiably Assess Center of Mass Kinematic Reconstruction

David J. Kelly, and Patrick M. Wensing

Abstract—The center of mass (COM) plays a fundamental role in human ambulation, but the redundant nature of the human body adds complexity to mathematically modeling its dynamics. Template models like the Bipedal Spring Loaded Inverted Pendulum (B-SLIP) and the Virtual Pivot Point (VPP) address this complexity by removing the redundancy while retaining desired salient characteristics, such as the COM evolution. However, template models for the COM during human walking have mostly been used for qualitative analysis due to issues such as overestimation of COM vertical displacement.

This paper considers a quantifiable template-based analysis of human walking by using an optimization framework to set the model parameter values for matching both explicitly and implicitly considered gait characteristics. Furthermore, it is shown that allowing the leg stiffness of the B-SLIP and VPP model to vary throughout the gait cycle better matches vertical COM trajectories with 54%-63% error reduction. These optimized template models show promise in retaining ground reaction force (GRF) information, which is not explicitly considered during the optimization process. Future work looks to incorporate these optimized trajectories as a reference for control of a lower-limb knee-ankle prosthesis.

I. INTRODUCTION

Ambulation underlies many activities in daily life. Individuals with a lower-limb amputation can experience a significant reduction in their ability to navigate surroundings and have higher risk of balance issues, negatively impacting quality of life [1]. Prostheses can help restore the mobility and capabilities that an individual had prior to amputation.

Passive prostheses harness mechanical design to replicate the missing limb. These devices see higher adoption rates among users due to higher affordability and easier adjustment [2]. However, these devices cannot actively react to perturbations (e.g., rough terrain) or inject work into the walking gait cycle, which is critical for ankle push-off [3]. Powered devices look to address these shortcomings through motorized joints. These devices require a robust controller that provides appropriate motor commands. The best controller for prostheses is still an open research topic, with two forms having been studied the most.

Position control focuses on joint progression while walking, commanding motors to match a reference trajectory [2]. High-fidelity joint angle tracking requires high stiffness to avoid oscillations, which can feel unnatural to the user [4]. Impedance control focuses on joint torques while walking, and is usually implemented via a finite state machine with



Fig. 1. Depiction of Virtual Pivot Point (VPP) model overlayed on top of a human walking with an Open Source Leg (OSL) prosthesis.

tunable stiffness, damping, and equilibrium parameters for each state [2]. This method may feel more natural to the user, however it can require tedious parameter tuning [4].

While both frameworks have seen successful use for walking, most implementations isolate the control and sensing to the instrumentation on the device itself. Sensors that are not isolated to the prosthesis can provide more information about the state of the user to enable greater synergy of control between user and device. Previous work has analyzed the importance of Center of Mass (COM) regulation for balance during walking [5], as well as its potential role in perturbation response [6]. External sensors would allow for explicit consideration of balance through COM kinematic feedback. However, the COM can only be estimated via methods like motion capture suits [7]. Likewise, the highly redundant nature of the human body adds complexity for modeling COM dynamics.

This complexity motivates template models, reduced-order mathematical models designed to eliminate the complexity and redundancy in a system while retaining the desired salient characteristics of it. For the COM during human walking, two popular template models are the Bipedal Spring-Loaded Inverted Pendulum (B-SLIP) [8] and Virtual Pivot Point (VPP) [9]. Previous work with these models has highlighted their qualitative agreement with COM trajectory and ground reaction force (GRF) profiles during walking when tuning parameters to generate stable cyclic gaits [10].

A common critique for the quantitative accuracy of these models is the overestimation of vertical COM displacement throughout the gait cycle [10]. The B-SLIP and VPP are energetically conservative without control input, however walking is not an energetically conservative task [3]. The overestimation of the vertical COM trajectory seen in these template models may be influenced by the use of a constant

^{*}This work was funded by the National Science Foundation Award CMMI-1943703

^{*}All authors are with the Department of Aerospace and Mechanical Engineering, University of Notre Dame, 365 Fitzpatrick Hall of Engineering, Notre Dame, Indiana dkelly@nd.edu

leg stiffness. Previous work has looked at varying the stiffness of the B-SLIP model via control inputs [11], however that work focused on expanding the space of stable walking gaits for the model, rather than fitting human walking data.

In this work, it is demonstrated that these models may be pushed toward quantitative analysis of human locomotion through incorporation of actuation via varying leg stiffness and the use of optimization methods. The contributions of this paper include a quantitative analysis of fitting the COM trajectory for the B-SLIP and VPP models to human walking data, as well as quantifying GRF profile matching and gait phase timings between the models and human data. This quantification framework is envisioned to enable the future use of optimized template models to track COM progression for balance during walking, while mapping the resulting GRF profile to appropriate torque commands for a lower-limb prosthesis like the Open Source Leg [12], (Fig. 1).

The rest of this paper is structured as follows: Sec. II details the dynamics of the B-SLIP and VPP models, with Sec. III outlining the optimization framework applied to these models. The optimization results are provided in Sec. IV, with discussion regarding these results in Sec. V. Implications and limitations of this work are summarized in Sec. VI.

II. MODEL DYNAMICS

The B-SLIP and VPP models used in this paper draw heavy inspiration from [8] and [9], respectively. This work uses a different axis for measuring leg and torso angles, which alters trigonometric conventions for the dynamics. A gait cycle for this work consists of two instances of both legs supporting the body (double support, DS) and two instances of the body vaulting over a single leg (single support, SS). A full gait cycle begins with touchdown of one leg and ends with the subsequent touchdown of that same leg.

In the B-SLIP model, a point mass, m, is located at the hip and balanced on massless Hookean springs with spring coefficient, k, and nominal length, ℓ_0 , as depicted in Fig. 2. The compression of the leg generates a spring force, $F_{\rm s}$, acting along the leg and through the point mass. This force represents the total ground reaction force (GRF), $F_{\rm GRF}$.

In the VPP model, the point mass is replaced with a rigid body trunk has a moment of inertia, J, as depicted in Fig. 3. The COM is offset from the hip by a distance, $r_{\rm h}$. To regulate trunk orientation, ϕ , a hip torque, τ , is applied to generate a reactionary force, $F_{\rm N}$, that is normal to the leg. Combining $F_{\rm N}$ and $F_{\rm s}$ results in $F_{\rm GRF}$ whose line of action intersects a virtual point (VP) a distance, $r_{\rm VP}$, above the COM. The hip, COM, and VP all lie along the axis aligned with ϕ .

A. Dynamic Formulation

The state variables of both models include the fore/aft and vertical position, (x, z) and velocity, (\dot{x}, \dot{z}) , of the COM, as well as the stiffness coefficient, $(\dot{k}_{\rm r}, \dot{k}_{\rm f})$, where $(\cdot)_{\rm r}$ and $(\cdot)_{\rm f}$ denotes rear and front leg, respectively. The VPP model also tracks the orientation and angular velocity, $(\phi, \dot{\phi})$, of the trunk. The stiffness coefficients are included as states such that the rates of change of the stiffness coefficients, $\dot{k}_{\rm r}$ and $\dot{k}_{\rm f}$,

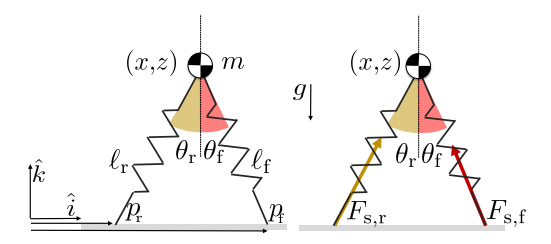


Fig. 2. The B-SLIP model with pertinent variables and parameters noted.

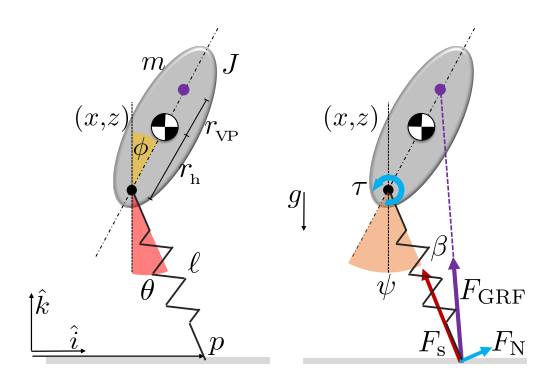


Fig. 3. The VPP model with pertinent variables and parameters noted.

become control variables. This extension effectively prevents discrete jumps in leg stiffness between time instances, which results in a smoother GRF profile. The state vector is then $\mathbf{s} = \begin{bmatrix} x \ z \ \dot{x} \ \dot{z} \ k_{\mathrm{r}} \ k_{\mathrm{f}} \end{bmatrix}^{\top} \text{ and } \mathbf{s} = \begin{bmatrix} x \ z \ \dot{\phi} \ \dot{k}_{\mathrm{r}} \ k_{\mathrm{f}} \end{bmatrix}^{\top} \text{ for the B-SLIP and VPP model, respectively.}$

The spring force for a given leg is calculated as

$$F_{s,i} = k_i(\ell_0 - \ell_i) \tag{1}$$

where ℓ_i is the current length of the leg and $i \in \{r, f\}$. Leg length is geometrically calculated based on foot position, p_i , and hip position. Hip position coincides with COM position for the B-SLIP model, and is found for the VPP using

$$x_{\rm h} = x - r_{\rm h} \sin(\phi)$$

$$z_{\rm h} = z - r_{\rm h} \cos(\phi).$$
 (2)

The B-SLIP fore/aft and vertical forces are determined using

$$F_{\mathbf{x},i} = F_{\mathbf{s},i} \sin(\theta_i) = F_{\mathbf{s},i} \frac{x_{\mathbf{h}} - p_i}{\ell_i}$$

$$F_{\mathbf{z},i} = F_{\mathbf{s},i} \cos(\theta_i) = F_{\mathbf{s},i} \frac{z_{\mathbf{h}}}{\ell_i}.$$
(3)

With gravity, g, the B-SLIP dynamics are

$$\frac{\mathrm{d}}{\mathrm{d}t} \begin{bmatrix} \dot{x} \\ \dot{z} \\ k_{\mathrm{r}} \\ k_{\mathrm{f}} \end{bmatrix} = \begin{bmatrix} \frac{1}{m} \sum_{i} F_{\mathrm{x},i} \\ \frac{1}{m} \sum_{i} F_{\mathrm{z},i} - g \\ \dot{k}_{\mathrm{r}} \\ \dot{k}_{\mathrm{f}} \end{bmatrix}$$
(4)

where only one force is present in SS and two in DS.

The VPP model dynamics require a few more calculations. By defining the angle between the leg and the trunk axis as $\psi_i = \theta_i + \phi$, the desired hip torque is found using

$$\tau_{i} = F_{s,i} \ell_{i} \tan(\beta_{i})$$

$$\tan(\beta_{i}) = \frac{(r_{h} + r_{VP}) \sin(\psi_{i})}{\ell_{i} + (r_{h} + r_{VP}) \cos(\psi_{i})}.$$
(5)

The VPP fore/aft and vertical forces are determined using

$$F_{x,i} = F_{s,i} \sin(\theta_i) - \frac{\tau_i}{\ell_i} \cos(\theta_i) = F_{s,i} \frac{x_h - p_i}{\ell_i} - \tau_i \frac{z_h}{\ell_i^2}$$

$$F_{z,i} = F_{s,i} \cos(\theta_i) + \frac{\tau_i}{\ell_i} \sin(\theta_i) = F_{s,i} \frac{z_h}{\ell_i} - \tau_i \frac{x_h - p_i}{\ell_i^2}.$$
 (6)

In total, the VPP model dynamics are then given by

$$\frac{\mathrm{d}}{\mathrm{d}t} \begin{bmatrix} \dot{x} \\ \dot{z} \\ \dot{\phi} \\ k_{\mathrm{r}} \\ k_{\mathrm{f}} \end{bmatrix} = \begin{bmatrix} \frac{1}{m} \sum_{i} F_{\mathrm{x},i} \\ \frac{1}{m} \sum_{i} F_{\mathrm{z},i} - g \\ \frac{1}{J} \sum_{i} (\tau_{i} - F_{\mathrm{x},i} r_{\mathrm{h}} \cos(\phi) + F_{\mathrm{z},i} r_{\mathrm{h}} \sin(\phi)) \\ \dot{k}_{\mathrm{r}} \\ \dot{k}_{\mathrm{f}} \end{bmatrix}.$$
(7)

III. OPTIMIZATION FRAMEWORK

A public data set of subjects walking on a treadmill was used for this work [13]. The subjects were tracked with a motion capture system, with force plates integrated into the treadmill. The COM data was fitted to a high order polynomial (order 20 and 25 for fore/aft and vertical, respectively) to interpolate values during the optimization. Since GRF data was only used post-optimization, spline interpolation using the optimized time values was conducted.

An optimization framework was designed to determine the variables of the template model that would fit the COM trajectory of the template models to walking data as closely as possible. Trajectory optimization is the process of optimizing control variables of a dynamic system relative to some cost function and constraints [14]. The primary goals of the optimization formulation were to a) best fit the template models to human COM walking data while b) maintaining a highly generalized formulation to mitigate solution overshaping. The optimization formulation used in this work was implemented in Matlab R2020b leveraging the CasADi and IPOPT frameworks [15], [16].

A multishooting method with Runge-Kutta 4th Order numerical integration and a 4th Order Gauss-Radau collocation method were considered for the transcription [14]. Ultimately, collocation was used due to its generally faster convergence and comparable results to multishooting. Each phase of the gait cycle was discretized into N=25 finite elements with M=4 collocation points per finite element. The optimization was run over a four-phase gait cycle (4NM) total points) with respect to the state variables, $\mathbf{S} = \begin{bmatrix} \mathbf{s}_1 \ \mathbf{s}_2 \ \dots \ \mathbf{s}_{4NM} \end{bmatrix}$, and non-state control variables, $\mathbf{U} = \begin{bmatrix} \mathbf{u}_1 \ \mathbf{u}_2 \ \dots \ \mathbf{u}_{4NM} \end{bmatrix}$. The mathematical formulation for the optimization is

$$\min_{\mathbf{S}, \mathbf{U}} \quad \sum_{j=1}^{4NM} \|\mathbf{y}_{j} - \mathbf{y}_{\text{hum}, j}\|^{2}$$
s.t.
$$\mathbf{h}_{\text{col}}(\mathbf{S}, \mathbf{U}) = 0,$$

$$\mathbf{g}(\mathbf{S}, \mathbf{U}) \leq 0,$$

$$\mathbf{W}_{\text{L}} \leq \mathbf{g}_{\text{b}}(\mathbf{S}, \mathbf{U}) \leq \mathbf{W}_{\text{U}}$$
(8)

where $\mathbf{y} = \begin{bmatrix} x \ z \end{bmatrix}^{\top}$ and $\mathbf{y}_{\text{hum}} = \begin{bmatrix} x_{\text{hum}} \ z_{\text{hum}} \end{bmatrix}^{\top}$ at each time instant, \mathbf{h}_{col} are equality and collocation constraints, \mathbf{g} are

inequality constraints, and g_b is used to set bounds on the variables. The collocation constraints ensure the propagation of each element/collocation point aligns with the subsequent element/point, and enforces consistent transitions between phases that respect the dynamics (e.g., foot position of leg at the start of SS is at the foot position of lead leg at the end of DS). The inequality constraints ensure that variables maintain expected behaviors (e.g., COM vertical velocity is negative at the start of DS, vertical GRF magnitudes are never negative). The objective is simply a running sum of the squared residuals between the optimized and experimental fore/aft and vertical positions of the COM.

The non-state control variables, \mathbf{u} , consist of variables chosen once per gait phase as well as some that are chosen continuously across each gait phase. For DS and SS, each gait phase includes a variable for its time duration, $t_{\rm f}$, and the starting positions, p_i , of each stance foot (enforcing no foot slip). The rate of change in spring stiffness, k_i , is chosen independently at each collocation point. For the DS phase, the touchdown angle, $\theta_{\rm TD}$, of the front leg is optimized as an initial condition for the phase. The nominal leg length, ℓ_0 , is the same across all phases.

The highly nonlinear model dynamics prevent global optimum guarantees. To help mitigate convergence to unwanted local optima, several variables were seeded with data from the walking experiments as initial guesses. This was done for the COM position and velocity at each time instant, the gait phase durations, and the nominal leg length.

IV. RESULTS

Three metrics were created to analyze how each template model variation fit subject data. The root mean squared error (RMSE) between the COM of the optimized template model and subject data at each time instance, $\epsilon_{\rm C}$, directly correlates to the objective function, and is non-dimensionalized with the measured leg length of the subject. The RMSE between the vertical GRF of the optimized template model and subject data at each time instance, $\epsilon_{\rm G}$, measures retention of salient characteristics not explicitly considered in the optimization, and is non-dimensionalized with the bodyweight of the subject. The RMSE between the phase durations of the optimized template model and subject data, $\epsilon_{\rm t_f}$, also measures salient characteristic retention with units of seconds.

The optimization framework was run for three sets of analysis. The first analysis focused on which template model variation best fit explicitly and implicitly considered gait characteristics. This process optimized four template variations for three separate gait cycles at a subject's preferred walking speed. The first two variations were the B-SLIP and VPP model with an optimized constant stiffness, analogous to previous work in literature. This was accomplished by constraining $\dot{k}_i = 0$. The third and fourth variations were the B-SLIP and VPP model with varying stiffness. Models appended with (C) and (V) denote constant and varying stiffness, respectively. Table I lists the preset parameters for the VPP model. The VP parameter was based on previous work that suggested its presence during SS but not DS [17].

TABLE I
TEMPLATE MODEL PARAMETERS

Parameter	Definition	Preset Value		
$r_{ m h}$	Distance between	0.1 m		
	COM and Hip			
[DS SS] $r_{\rm VP}$	Distance between	[0 0.15] m		
	COM and VP			
J	moment of inertia	4.58 kg m^2		
g	gravity constant	9.81 m/s ²		

All template model variations were optimized for Subject 04 from [13]. Subject 04 was chosen because their preferred walking speed is in the middle of preferred walking speeds for all available subjects, and is close to average human walking speed [5]. Table II contains the measured leg length, preferred walking speed, and bodyweight for Subject 04.

The second analysis used walking data from Subject 04 not at their preferred walking speed. This analysis focused on the effect walking at slower (0.71 m/s) and faster (1.69 m/s) speeds had on model fitting. This analysis was conducted for three separate gait cycles, and only used the model that performed best in the first analysis.

The third analysis optimized the same model as the second analysis for subjects whose preferred walking speeds were different from Subject 04. The parameters for these subjects are listed in Table II. This analysis focused on the effect slower and faster *preferred* walking speeds had on model fitting, and was completed for three separate gait cycles.

Fig. 4-7 visualize the results of the first analysis. Since overestimation of vertical COM displacement is a common critique of these template models, the vertical COM trajectories for each template model optimized for Subject 04 were graphed with the experimental vertical COM trajectory in Fig. 4. Markers to denote the instances of gait phase transitions are included. Since the main form of optimized control is via leg stiffness, the stiffness profile for each template model is graphed in Fig. 5. To analyze the retention of important walking features such as vertical GRF profiles, the post-optimization calculation of the vertical GRFs for each model are overlayed on the experimental vertical GRF data in Fig. 6. The quantifiable assessment of the template model fitting to human data is illustrated in Fig. 7, with data regarding solve times and status provided in Table III.

Based on the quantification metrics, the optimized VPP (V) model best captured explicit and implicit characteristics of human walking, and was chosen for conducting the second and third analyses. For these analyses, the resulting quantification metrics were averaged across the three optimized gait cycles for sake of brevity in reporting. Table IV provides the resulting averaged metric performances of the VPP (V) model at different walking speeds for Subject 04. Table V provides the resulting averaged metric performances of the VPP (V) model at preferred walking speeds for multiple subjects *in order of increasing preferred walking speed*.

V. DISCUSSION

The overestimation and overall fit of vertical COM displacement is significantly improved for both models when

TABLE II
SUBJECT PARAMETER DATA

Subject	Leg Length [m]	Weight [kg]	Preferred Speed [m/s]
04	0.94	61.05	1.30
12	0.78	48.80	1.05
13	0.85	95.40	1.02
15	0.92	89.30	1.54
18	0.86	59.30	1.26
21	0.91	61.50	1.42

optimized with varying leg stiffness. These results are evident qualitatively in Fig. 4 and quantitatively in Fig. 7. This finding suggests that models require some form of non-conservative energy component to agree quantitatively with human data. The work in [18] agrees with this conclusion, where a damper was incorporated to modulate the apparent leg stiffness in a spring-mass model.

From Fig. 5, it appears that the constant stiffness models chose an average value from the stiffness profile of the varying models. These stiffness values tend to be smaller than what has been reported from other work, [10]. However, in [10] the gait-event timings and fore-aft distance for the B-SLIP model were shorter than observed in human data. These results align with what is expected for higher leg stiffness, suggesting that the smaller values reported here may better capture these aspects of human walking behavior.

It is important to note that the optimized leg stiffness is a low-complexity linear abstraction of biomechanical properties of human walking. Energy absorption and injection from the coordinated firing of leg muscles and actuation of joints, [3], is essentially lumped into the single stiffness component. While these leg stiffness values do not have a direct correlation to specific aspects of human biomechanics, the abstraction does appear to highlight the importance of including some non-conservative component to these models.

The improvement to human data fitting appears to expand beyond *explicitly* considered characteristics. The varying stiffness models better fit to GRF profiles than the constant stiffness models, seen qualitatively in Fig. 6 and quantitatively in Fig. 7. The retention is particularly notable in the ability to capture the asymmetry of the second M-profile, suggesting that joint-level variables (i.e., torques) can be predictably realized when focusing on task-level variables such as COM. This observation aligns with the task-level perturbation response suggested in [6]. The ability to work with task-level parameters without sacrificing joint-level information supports the inclusion of sensors not isolated to the device into the control of lower extremity prostheses.

Similar results arise for gait phase durations as seen in Fig. 7. The constant stiffness models consistently saw larger disparity in the gait phase durations, further aligning with the results in [18]. The VPP (V) model performed the best in all three trials, suggesting that the combination of some non-conservative component with incorporation of trunk dynamics may retain more characteristics of human walking. The results hint at trade-offs between complexity of the models and available information in the models.

Optimizing the VPP (V) model for gait speeds away

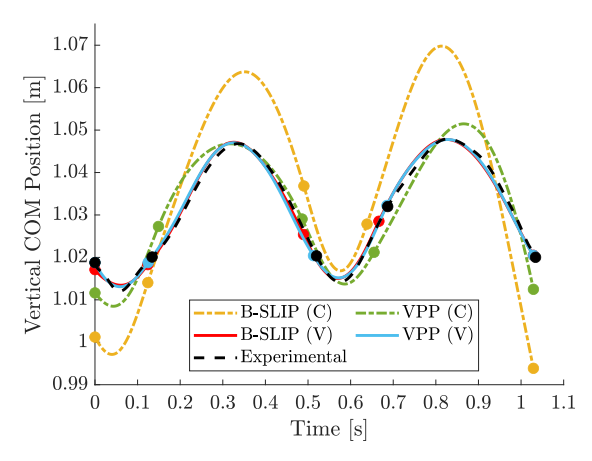


Fig. 4. Vertical COM trajectory with respect to time for each template variation compared to the experimental COM data for a single gait cycle of Subject 04 at their preferred walking speed. The (C) and (V) denote models with constant and varying leg stiffness, respectively.

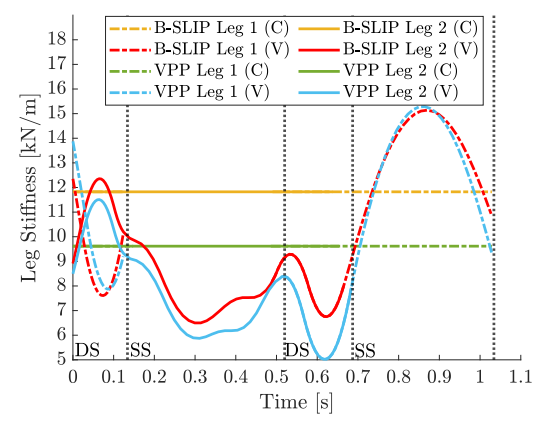


Fig. 5. Leg stiffness with respect to time for each template model variation for a single gait cycle of Subject 04 at their preferred walking speed. The (C) and (V) denote models with constant and varying leg stiffness, respectively.

from the preferred walking speed of Subject 04 showed mixed results. A good fit to COM data is maintained, while increased $\epsilon_{\rm G}$ for slower walking and increased $\epsilon_{\rm t_f}$ for faster walking optimization is observed in Table IV. The increase in $\epsilon_{\rm G}$ may be due to a more irregular vertical COM trajectory at slower walking for Subject 04. A plateau before peak vertical COM height during SS resulted in leg stiffness oscillations that propagated into oscillations in the GRFs. The increase in $\epsilon_{\rm t_f}$ may be due to the shorter DS duration for the human data. The VPP model favors a longer DS phase, which is inherently more stable than SS phase [17].

Optimizing the VPP (V) model for subjects at different preferred walking speeds aligned with results for Subject 04 at their preferred walking speed, as reported in Table V. The overall quantification metric results for all subjects suggest that the optimization framework is applicable to a range of preferred walking speeds. The potential degradation seen in Table IV may be due to amplified irregularity in gait when not walking at one's preferred speed, a trend reported in [19].

As anticipated, the variable stiffness models require more iterations and time to complete their optimization compared

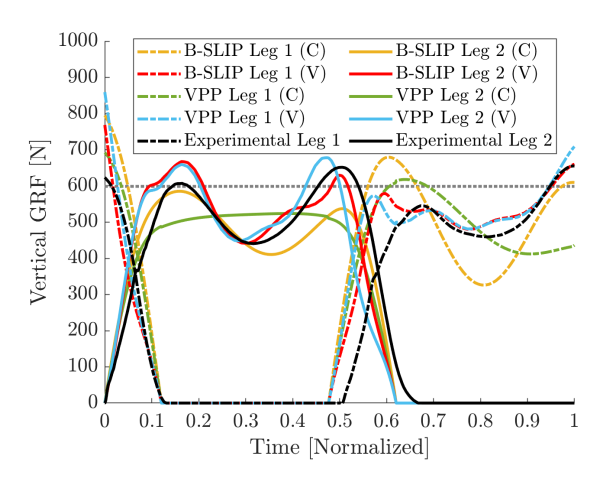


Fig. 6. Vertical GRF profile with respect to normalized time for each template variation compared to the experimental GRF data for a single gait cycle of Subject 04 at their preferred walking speed. The (C) and (V) denote models with constant and varying leg stiffness, respectively.

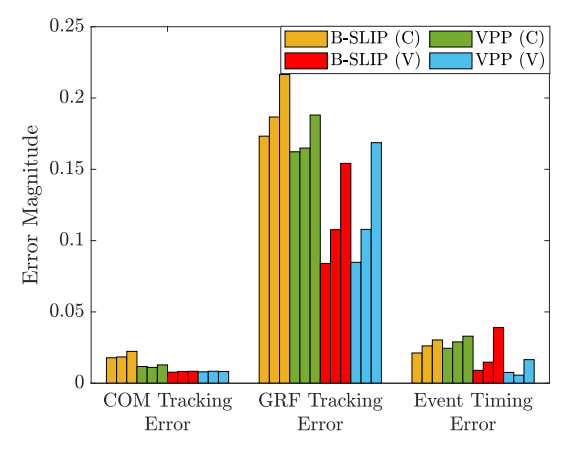


Fig. 7. Quantification metrics for each template variation based on three separate gait cycles for Subject 04 at their preferred walking speed. The (C) and (V) denote models with constant and varying leg stiffness, respectively.

to their constant stiffness counterparts (Table III). All except one constant stiffness B-SLIP gait cycle terminated with at least Acceptable status. While the solve times rule out on-line considerations, the off-line optimized models can be used as reference trajectories to track how real-time COM data compares to expected behavior. This provides a baseline for determining if the GRF profile from the optimized model is appropriate to replicate with a powered lower-limb prosthesis. Future work will focus on developing the mapping between GRF and joint torque commands to be implemented on the Open Source Leg (OSL), which can be commanded to imitate impedance behavior [20].

The current framework does have some limitations. While trends for each template variation have held for most optimized gait cycles, irregularities in an isolated gait cycle can cause issues. This sensitivity is being addressed in ongoing work by optimizing over an averaged gait cycle for a subject. The end points of the gait cycle show the largest disparity in model fitting. This disparity is being mitigated by optimizing over multiple gait cycles and analyzing the middle gait cycle(s). The highly nonlinear characteristic of these

TABLE III

OPTIMIZATION SOLVER STATISTICS FOR SUBJECT 04 AT PREFERRED

WALKING SPEED

	B-SLIP		VPP	
	(C)	(V)	(C)	(V)
	369	888	194	355
Iterations	340	449	183	296
	358	432	187	263
Time [s]	14.88	115.55	16.19	26.51
	13.77	18.98	14.15	22.91
	12.63	18.13	14.67	17.99
Status	Failed	Optimal	Optimal	Acceptable
	Optimal	Acceptable	Optimal	Acceptable
	Optimal	Optimal	Optimal	Acceptable

 ${\it TABLE\ IV} \\ {\it VPP\ Fit\ Quantification\ at\ Various\ Gait\ Speeds\ for\ Subject\ 04}$

	Slow	Preferred	Fast
	0.71 m/s	1.30 m/s	1.69 m/s
ϵ_{C}	0.0076	0.0080	0.0098
$\epsilon_{ m G}$	0.1726	0.0848	0.1096
$\epsilon_{\mathrm{t_f}}$ [s]	0.0098	0.0076	0.0176

template models may result in the solver converging to a local optimum that is not an acceptable fit to the human data. Future work looks to incorporate a perturbation method to adjust the seeded initial guesses to avoid these local optima.

VI. CONCLUSION

In this work, it was shown that template models have the capability to improve quantifiable fit to human COM data during human walking via trajectory optimization. By varying the leg stiffness of the models throughout the gait cycle, a more accurate fit of the COM trajectory was achieved. Both the B-SLIP and VPP models were able to retain salient characteristics of human walking like GRF profiles that were not explicitly accounted for in the optimization framework. The VPP model showed more initial promise in retaining phase duration information than the B-SLIP model, and demonstrated that quantifiably fitting to walking speeds away from a person's preferred speed may be feasible.

Future work will look to address the limitations of undesired local optima, gait cycle endpoint disparity, and single vs. average gait cycle data. This work will also continue to expand the analysis of different preferred walking speeds to understand the range of speeds this optimization framework may work for. Continued analysis of performance for gait cycles away from preferred walking speed will be helpful for determining the robustness of the models to various walking conditions. Finally, this work will be used in the next steps of task-level control by using the GRF profiles obtained from the optimized template models and mapping those forces to individual joint torques of a lower-limb prosthesis.

REFERENCES

 W. C. Miller, M. Speechley, and B. Deathe, "The prevalence and risk factors of falling and fear of falling among lower extremity amputees," *Archives of physical medicine and rehabilitation*, vol. 82, no. 8, pp. 1031–1037, 2001.

TABLE V

VPP FIT TO SUBJECTS WITH DIFFERENT PREFERRED WALKING SPEEDS

	Slower		Similar	Similar Faster	
	Subj. 13	Subj. 12	Subj. 18	Subj. 21	Subj. 15
ϵ_{C}	0.0082	0.0085	0.0080	0.0090	0.0096
$\epsilon_{ m G}$	0.1011	0.1132	0.1370	0.1358	0.1498
$\epsilon_{\mathrm{t_f}}$ [s]	0.0070	0.0087	0.0110	0.0077	0.0104

- [2] M. R. Tucker, J. Olivier, A. Pagel, H. Bleuler, M. Bouri, O. Lambercy et al., "Control strategies for active lower extremity prosthetics and orthotics: a review," *Journal of neuroengineering and rehabilitation*, vol. 12, no. 1, pp. 1–30, 2015.
- [3] F. E. Zajac, R. R. Neptune, and S. A. Kautz, "Biomechanics and muscle coordination of human walking: part ii: lessons from dynamical simulations and clinical implications," *Gait & posture*, vol. 17, no. 1, pp. 1–17, 2003.
- [4] C. Ferreira, L. P. Reis, and C. P. Santos, "Review of control strategies for lower limb prostheses," in *Robot 2015: Second Iberian Robotics Conference*. Springer, 2016, pp. 209–220.
- [5] L. Tesio and V. Rota, "The motion of body center of mass during walking: a review oriented to clinical applications," Frontiers in neurology, p. 999, 2019.
- [6] S. A. Safavynia and L. H. Ting, "Long-latency muscle activity reflects continuous, delayed sensorimotor feedback of task-level and not jointlevel error," *Journal of neurophysiology*, vol. 110, no. 6, pp. 1278– 1290, 2013.
- [7] M. Schepers, M. Giuberti, and G. Bellusci, "Xsens mvn: Consistent tracking of human motion using inertial sensing," *Xsens Technol*, vol. 1, no. 8, 2018.
- [8] H. Geyer, A. Seyfarth, and R. Blickhan, "Compliant leg behaviour explains basic dynamics of walking and running," *Proceedings of the Royal Society B: Biological Sciences*, vol. 273, no. 1603, pp. 2861– 2867, 2006.
- [9] M. N. Vu, J. Lee, and Y. Oh, "Control strategy for stabilization of the biped trunk-slip walking model," in 2017 14th International Conference on Ubiquitous Robots and Ambient Intelligence (URAI). IEEE, 2017, pp. 1–6.
- [10] S. W. Lipfert, M. Günther, D. Renjewski et al., "A model-experiment comparison of system dynamics for human walking and running," *Journal of theoretical biology*, vol. 292, pp. 11–17, 2012.
- [11] L. C. Visser, S. Stramigioli, and R. Carloni, "Bipedal locomotion using variable stiffness actuation," arXiv preprint arXiv:1706.00339, 2017.
- [12] A. F. Azocar, L. M. Mooney, J.-F. Duval, A. M. Simon, L. J. Hargrove, and E. J. Rouse, "Design and clinical implementation of an opensource bionic leg," *Nature biomedical engineering*, vol. 4, no. 10, pp. 941–953, 2020.
- [13] C. A. Fukuchi, R. K. Fukuchi, and M. Duarte, "A public dataset of overground and treadmill walking kinematics and kinetics in healthy individuals," *PeerJ*, vol. 6, p. e4640, 2018.
- [14] L. T. Biegler, Nonlinear programming: concepts, algorithms, and applications to chemical processes. SIAM, 2010.
- [15] J. A. Andersson, J. Gillis, G. Horn, J. B. Rawlings, and M. Diehl, "Casadi: a software framework for nonlinear optimization and optimal control," *Mathematical Programming Computation*, vol. 11, no. 1, pp. 1–36, 2019.
- [16] L. T. Biegler and V. M. Zavala, "Large-scale nonlinear programming using ipopt: An integrating framework for enterprise-wide dynamic optimization," *Computers & Chemical Engineering*, vol. 33, no. 3, pp. 575–582, 2009.
- [17] J. Vielemeyer, R. Müller, N.-S. Staufenberg, D. Renjewski, and R. Abel, "Ground reaction forces intersect above the center of mass in single support, but not in double support of human walking," *Journal* of biomechanics, vol. 120, p. 110387, 2021.
- [18] S. Kim and S. Park, "Leg stiffness increases with speed to modulate gait frequency and propulsion energy," *Journal of biomechanics*, vol. 44, no. 7, pp. 1253–1258, 2011.
- [19] N. Sekiya, H. Nagasaki, H. Ito, and T. Furuna, "Optimal walking in terms of variability in step length," *Journal of Orthopaedic & Sports Physical Therapy*, vol. 26, no. 5, pp. 266–272, 1997.
- [20] J.-F. Duval and H. M. Herr, "Flexsea: flexible, scalable electronics architecture for wearable robotic applications," in 2016 6th IEEE International Conference on Biomedical Robotics and Biomechatronics (BioRob). IEEE, 2016, pp. 1236–1241.